An Analytical Model of Quadrotor Electrical Energy Consumption

Vadym Honcharenko
Department of Applied Mathematics, Kharkiv National University of Radio Electronics, Kharkiv, Ukraine
vadym.honcharenko@nure.ua (corresponding author)

Valentyn Yesilevskyi
Department of Applied Mathematics, Kharkiv National University of Radio Electronics, Kharkiv, Ukraine
valentyn.yesilevskyi@nure.ua

Received: 23 September 2025 | Revised: 29 December 2025 and 21 January 2026 | Accepted: 27 January 2026

 DOI: https://doi.org/10.48084/etasr.15062

ABSTRACT

The electrical energy consumption of a quadrotor is a critical factor limiting mission duration. Existing models rely on experimental data for specific configurations or simplify the underlying processes, limiting generalization and accuracy. This study presents a generalizable and accurate analytical model for estimating the electrical energy consumption of a quadrotor based solely on manufacturer-provided parameters, without requiring additional parameter identification or aerodynamic assumptions. The model integrates a second-order Thevenin battery equivalent circuit, an Electronic Speed Controller (ESC), and a first-order motor model that accounts for nonlinear voltage drop effects and load-dependent efficiency. Model input variables are limited to rotor angular speed and torque, and all model parameters are known component specifications. The model decouples energy estimation from aerodynamic models, enabling integration into various simulations and control systems. Simulation results demonstrate that the proposed model produces more accurate results than simplified models, allowing for a reduction of up to 21% relative to a constant-voltage baseline, and it matches motor-current curves from public bench measurements. The model offers practical benefits for UAV mission planning, energy-aware control algorithms, and research on drone endurance optimization.

Keywords-mathematical modeling; energy consumption; quadrotor; battery model

I. INTRODUCTION

Quadrotors are now utilized in various practical applications, including agriculture [1], civil engineering [2], environmental monitoring [3], search and rescue operations, and numerous other fields. However, endurance remains the primary constraint due to the finite energy capacity of Li-ion batteries. Because simply adding batteries degrades mass efficiency, energy-aware planning requires a tractable, component-level model of electrical consumption.

Despite their popularity and advantages, quadrotors face a critical limitation: finite onboard energy resources. Since adding batteries increases weight disproportionately and reduces efficiency, developing energy-efficient flight techniques is essential. This is a nontrivial task due to the quadrotor's kinematic complexity. Therefore, comprehensive analysis and optimization of energy consumption are crucial for enhancing the endurance and efficiency of quadrotors. For such analysis, a mathematical model of the energy consumption process is necessary.

A. Literature Review

Energy consumption modeling for quadrotors is crucial for optimizing flight endurance, mission planning, and control. Existing approaches to this problem can be broadly classified into empirical (data-driven) and analytical (physics-based) models. Data-driven approaches include a time-series LSTM energy consumption model [4], an ensemble stacking power estimation model [5], and an empirical polynomial model built from battery measurements across UAV maneuvers [6]. While these models demonstrate low error under specific conditions, they heavily rely on experimental datasets and lack generalization to different UAV configurations or mission profiles. Each new drone setup typically requires retraining or parameter re-identification, which limits scalability and practical deployment. Simple analytical power models use a single physical principle. Examples include an endurance model grounded in rotorcraft theory [7], an energy consumption model based on kinematic acceleration and deceleration [8], and a blade-centered aerodynamic power consumption model [9, 10]. These models simplify the system by focusing on macroscopic variables like speed, altitude, and

payload. However, they often neglect the detailed electromechanical characteristics of the propulsion system, especially the effects of dynamic load changes and internal electrical losses. Furthermore, their reliance on predefined flight regimes or hovering assumptions limits their applicability to complex mission profiles.

Another group of energy consumption models couples aerodynamic (blade-element theory or thrust/torque-coefficient) with electrical sub-models of the propulsion chain, which improves control over simulation variables and theoretical generalization. For instance, in [11], the proposed model incorporated a simple battery model, conduction losses, back electromotive force loss, and a linear model of mechanical loss. Authors in [12-16] employed more complex electromechanical rotor models; thereby coupling the electrical and mechanical aspects of the simulations. Specifically, authors in [12] deployed an electromechanical model with a motor efficiency regression function derived from empirical data. Authors in [13] added a modified Shepherd Li-ion battery model, accounted for thrust and wind correction, and utilized a motor efficiency function. Authors in [14] utilized an approach analogous to [13], but with different submodels, and validated the quadrotor energy model via Monte-Carlo uncertainty propagation, quantifying sensitivity to parameter and wind variations. In [15], an extensive blade-element theory-based model was coupled with an electro-mechanical rotor model, without accounting for other electrical components. Authors in [16] proposed an integrated electrical model that covers the propeller, motor, ESC, and battery, incorporating armature reaction and a simple thermal effect; however, it required per-motor experimental identification. However, these models typically demand custom experiments to identify parameters, or they simplify transient and nonlinear effects to maintain computational efficiency.

The critical review of the literature reveals several unresolved issues: the lack of generalization in empirical models across UAV types and missions; the simplification or omission of electrical subsystem dynamics, particularly under nonlinear loads; the coupling of energy models with aerodynamic and kinematic models, reducing modularity; and the dependence on hard-to-obtain experimental data or fitting procedures for parameter identification.

B. Study Contribution

In contrast to these approaches, the model proposed in this paper employs only datasheet-level parameters for all electrical components and explicitly separates the electrical submodel from the choice of an aerodynamic or kinematic model. This allows the same electrical parameterization to be reused across different mission profiles and trajectory generators without requiring additional parameter identification. The main contributions of this work are:

- A discrete-time analytical model of the quadrotor electrical power consumption that uses only manufacturer-provided parameters and does not require additional parameter identification.
- An integrated Electrical Propulsion System (EPS), which consists of the ESC and motor, providing a unified electrical description that can be directly coupled to external kinematic/aerodynamic simulators via rotor torque and angular speed inputs.
- Explicit accounting for the electrical consumption of the flight control system and payload.

II. BACKGROUND

Quadrotors (and multicopters in general) are powered by a DC battery that supplies: (i) N identical electrical propulsion branches (ESC + BLDC motor + propeller) and (ii) auxiliary onboard systems (flight controller and payload). The goal of this paper is to model the electrical energy consumption of the entire platform while maintaining a modular and compatible electrical model that can be integrated with any external aerodynamic/kinematic simulator.

A. System Architecture, Notation, and Interfaces

Figure 1 illustrates the proposed structural model for electrical energy consumption. The diagram explicitly shows each submodel's inputs, parameters, states, and outputs, as well as the interconnections between submodels.

The current study uses a discrete-time model with an index k and a sampling interval Δt. The multicopter is modeled as N identical EPS branches indexed by $i \in \{1,\ldots,N\}$, for quadrotors $N = 4$. Each EPS branch has a propeller torque $Q_{F,k,i}[N \cdot m]$ and angular speed $\omega_{k,i}[rpm]$ as inputs. Also the model inputs are the payload $I_{P,k}$ and the flight control system $I_{FCS,k}$ load currents.

The main electrical variables of the model are:

- Battery terminal voltage $V_{B,k}$ and current $I_{B,k}$.
- Motor AC voltage $V_{MAC,k,i}$ and current $I_{MAC,k,i}$.
- ESC loss current $I_{ESC,k,i}$ and motor DC load current $I_{MDC,k,i}$.

Another important model part is the battery states – State of Charge (SoC_k), short-term $V_{S,k}$ and long-term $V_{L,k}$ voltage drops.

B. Battery Model

In most quadrotor systems, lithium-ion batteries are the sole onboard energy source. As such, battery characteristics influence the aircraft's performance limits, endurance, and range. Due to the propulsion system's high energy demand, the limited energy storage capacity of the battery is the primary constraint on mission duration. Nevertheless, in many studies on endurance optimization, battery behavior is either oversimplified or represented abstractly through energy constraints without dynamic modeling. A lithium-ion battery's main properties [17] include nominal capacity $C_n[A \cdot s]$, which represents the energy stored when fully charged (typically provided by manufacturers in $\mathrm{mA \cdot h}$, but in formulas, it is expressed in $\mathrm{A \cdot s}$). The SoC is the ratio of available capacity

to nominal capacity. An open-circuit voltage V_{OC} is the battery's terminal voltage when no load is applied. It is well established that it decreases as SoC declines.

While some UAV energy models reduce the battery to a constant-voltage, capacity-limited source, such a simplification neglects the battery's load-dependent and nonlinear behavior, including: 1) the capacity effect – higher discharge currents reduce the usable energy output due to internal losses; 2) the voltage drop effect – terminal voltage decreases not only with SoC but also with higher instantaneous current loads; and 3) the dynamic response – the terminal voltage does not change instantaneously with current fluctuations, but transitions gradually based on previous load conditions.

These effects are especially significant in multicopter applications with frequent and rapid load changes. Although thermal effects are also relevant, they are excluded from this study for simplicity.

A wide range of Equivalent Circuit Models (ECMs) exists for lithium-ion batteries, each varying in complexity, accuracy, and parameter requirements. Among these, the second-order Thévenin model is widely recognized for its ability to simulate nonlinear voltage behavior and dynamic load response. It is well-suited for high-current, dynamic applications like UAVs.

This work adopts a second-order Thévenin ECM, based on [18], because it can model the critical effects influencing quadrotor energy consumption without requiring excessive computational resources. The battery model consists of two main components: 1) an open-circuit voltage source $V_{OC}(SoC_{k+1})$ that models the voltage as a function of SoC; and 2) an internal series resistance R_0 and two RC circuits R_S, C_S short-time and R_L, C_L long-time dynamic voltage responses. The battery model input is the terminal load current $I_{B,k}$.

The SoC is updated:

$$SoC_{k+1} = SoC_k - \frac{I_{B,k}}{C_n}\Delta t \quad (1)$$

The battery terminal voltage is then given by:

$$V_{B,k+1} = V_{S,k+1} + V_{L,k+1} - RI_{B,k} + V_{OC}(SoC_{k+1}) \quad (2)$$

$$V_{S,k+1} = V_{S,k} \cdot \exp\left(\frac{-\Delta t}{R_S C_S}\right) - I_{B,k} \cdot \left(\exp\left(\frac{\Delta t}{C_S}\right) - 1\right) \quad (3)$$

where $V_{S,k}$ is a short-term voltage drop.

$$V_{L,k+1} = V_{L,k} \cdot \exp\left(\frac{-\Delta t}{R_L C_L}\right) - I_{B,k} \cdot \left(\exp\left(\frac{\Delta t}{C_L}\right) - 1\right) \quad (4)$$

where $V_{L,k}$ is a long-time voltage drop.

During discharge, $V_{S,k}, V_{L,k}$ drop battery's open circuit voltage to its terminal values.

The RC parameters can be assumed constant across SoC for implementation efficiency without significantly affecting model accuracy [17]. The open-circuit voltage $V_{OC}(SoC)$ is modeled as a 7th-degree polynomial fit to empirical discharge data with coefficients $\{v_i\}_{i=0}^{7}$, as in [17]. The model parameters R_0, R_S, C_S, R_L, C_L may be obtained experimentally or sourced from manufacturer specifications.

This model accurately reflects the battery's nonlinear and time-dependent behavior. The empirical function $V_{OC}(SoC)$ is a monotonically decreasing nonlinear curve, while the two RC branches introduce exponential voltage dynamics in response to load changes. These nonlinearities make the battery the most influential source of variation in the overall energy consumption model. As a result, identical power demands under different SoC or transient conditions may correspond to significantly different current loads and discharge rates, influencing overall endurance.

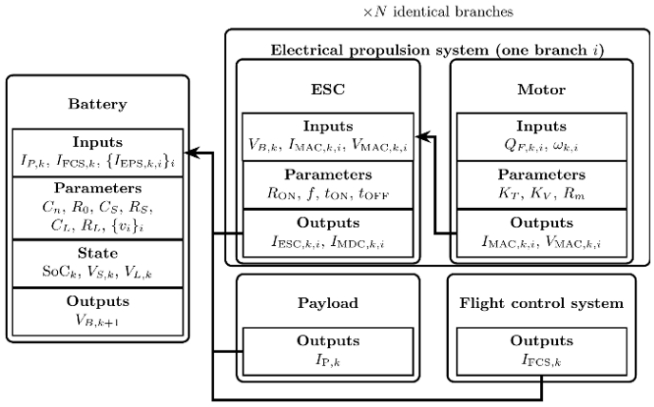

Fig. 1. Structural scheme of the proposed electrical energy consumption model.

C. Electronic Speed Controller Model

The ESC is a significant subsystem in quadrotor propulsion. It converts the battery's DC voltage $V_{B,k}$ into motor-side three-phase AC voltage $V_{MAC,k,i}$ via Pulse-Width Modulation (PWM) in order to drive brushless DC motors. The motor AC load current $I_{MAC,k,i}$ (per-phase RMS motor), is recalculated into DC $I_{MDC,k,i}$. ESC losses are represented as an additional loss power $P_{ESC,k,i}$ (or loss-equivalent current $I_{ESC,k,i}$). According to [19], ESCs typically achieve energy conversion efficiencies ranging from 80% to 99%, depending on load conditions and hardware specifications.

In this study, the ESC is modeled analytically by adopting the PWM conduction and switching-loss formulation reported in [16], which captures the essential loss mechanisms arising during PWM switching. The ESC output AC voltage $V_{MAC,k}$ is regulated by adjusting the PWM duty cycle $d_{k,i}$. The duty

cycle is calculated from the known battery voltage $V_{B,k}$ and the motor AC voltage $V_{MAC,k,i}$ using:

$$V_{MAC,k,i} = d_{k,i} V_{B,k,i} \quad (5)$$

Correspondingly, the motor input direct current $I_{MDC,k,i}$ and the motor alternating current $I_{MAC,k,i}$ are linked through the duty cycle as:

$$I_{MDC,k,i} = I_{MAC,k,i} d_{k,i} \sqrt{3} \quad (6)$$

The total power loss within the ESC $P_{ESC,k,i}$ comprises two primary components: conduction losses $P_{C,k,i}$ and switching losses $P_{SW,k,i}$ [16]:

$$P_{ESC,k,i} = P_{C,k,i} + P_{SW,k,i} \quad (7)$$

Conduction losses occur due to the internal MOSFET resistances R_{ON} and are quantified as:

$$P_{\mathrm{C,k},i} = d_{k,i} \cdot R_{ON} \cdot I_{MDC,k,i}^2 \quad (8)$$

Switching losses result from high-frequency transistor transitions between conductive states. These losses are calculated using the switching frequency f, the battery voltage, the battery current, and the MOSFET switching durations t_{ON} and t_{OFF}:

$$P_{SW,k,i} = \frac{1}{2} \cdot I_{MDC,k,i} \cdot V_{B,k,i} \cdot \left(t_{ON} + t_{OFF}\right) \cdot f \quad (9)$$

The required parameters can be obtained from manufacturer datasheets or through experimental procedures. Incorporating this detailed ESC loss model improves the accuracy of quadrotor energy consumption simulations.

D. Brushless Direct Current Motor Model

Brushless Direct Current (BLDC) motors are utilized in quadrotors due to their high efficiency, reliability, and precise controllability. They convert electrical energy into mechanical torque, driving propellers to generate the required lift and thrust forces.

Various BLDC motor models exist in the literature, ranging from highly detailed analytical representations to simplified empirical models. This study adopts a two-constant motor model [20] due to its balance of simplicity and accuracy. Furthermore, its parameters are available from standard motor specifications provided by manufacturers. This model uses two main parameters: the motor's speed constant $K_V[rpm/V]$ and the internal resistance R_m. Given the motor's torque $Q_{F,k,i}[N \cdot m]$ and angular speed $\omega_{k,i}[rpm]$, the motor model produces motor AC voltage $V_{MAC,k,i}$ and current $I_{MAC,k,i}$, which are then used by the ESC model (Figure 1).

The equation linking the generated mechanical torque $Q_{F,k,i}$ and the motor AC current $I_{MAC,k,i}$ is:

$$I_{MAC,k,i} = Q_{F,k,i} K_F \quad (10)$$

The equation linking the motor angular velocity $\omega_{k,i}$ and the motor terminal voltage $V_{MAC,k,i}$ is:

$$V_{MAC,k,i} = \frac{\omega_{k,i}}{K_V} + I_{MAC,k,i} R_m \quad (11)$$

The model implicitly includes mechanical losses such as friction, inertia, and other minor losses through the internal resistance parameter R_m, which can be empirically determined from manufacturer datasheets or controlled laboratory experiments. Due to their minimal impact at the operational scale of typical quadrotor motors, magnetic flux dynamics, inductance, and inertia effects are neglected [12]. Despite its simplicity, this two-constant ECM provides reliable predictions of motor performance under realistic quadrotor operating conditions and adequately reflects essential nonlinear effects such as load-dependent voltage drops and efficiency losses.

III. ENERGY CONSUMPTION MODEL

This section integrates the battery, ESC, and motor submodels into a single discrete-time analytical model, consistent with the input and calculation flow shown in Figure 1. The model maps the mechanical inputs $\left\{Q_{F,k,i}, \omega_{k,i}\right\}_{i=1}^{N}$ and auxiliary currents $\left(I_{P,k}, I_{FCS,k}\right)$ to the battery terminal current $I_{B,k}$ and the next step voltage $V_{B,k+1}$, thereby enabling the calculation of energy consumption for each subsystem and for the system as a whole.

A. Subsystem Coupling and Variable Propagation

At each time step we know: The battery terminal voltage $V_{B,k}$ and states SoC_k, $V_{S,k}$, $V_{L,k}$, computed at the end of the previous step, the mechanical inputs $\left\{Q_{F,k,i}, \omega_{k,i}\right\}_{i=1}^{N}$, and the auxiliary currents $\left(I_{P,k}, I_{FCS,k}\right)$. This enables calculating the load currents of every subsystem, next step battery terminal voltage $V_{B,k+1}$, and states.

Variable propagation and computation:

1. Convert the motor's mechanical inputs $\left\{Q_{F,k,i}, \omega_{k,i}\right\}_{i=1}^{N}$ to electrical outputs $\left\{I_{MAC,k,i}, V_{MAC,k,i}\right\}_{i=1}^{N}$ using (10) and (11).
2. Calculate the ESC duty cycle using (12), derived from (5):
$$d_{k,i} = V_{MAC,k,i} / V_{B,k} \quad (12)$$
3. Convert $\left\{I_{MAC,k,i}\right\}_{i=1}^{N}$ to $\left\{I_{MDC,k,i}\right\}_{i=1}^{N}$ using (6).
4. Calculate the EPS load current $I_{EPS,k,i}$ using (13) and (14), based on (7):
$$I_{ESC,k,i} = P_{ESC,k,i} / V_{B,k} \quad (13)$$

Overall, the electrical propulsion branch load current is the sum of the motor load current and the ESC loss current (14). ESC and motor submodels are coupled into a single EPS model block using:

$$I_{EPS,k,i} = I_{ESC,k,i} + I_{MDC,k,i} \quad (14)$$

5. Compute the total load current using (15), which connects all the subsystems into a single model. It combines propulsion system current $I_{EPS,k}$, payload current $I_{P,k}$, and flight control system current $I_{FCS,k}$. Payload and flight control system power load are typically time-dependent, but are simplified as constant values:

$$I_{B,k} = I_{P,k} + I_{FCS,k} + \sum_{i=1}^{N} I_{EPS,k,i} \quad (15)$$

6. The battery update uses $I_{B,k}$ to compute next time-step battery states and voltage with (1) – (4).

B. Model Summary, Assumptions, and Limitations

The present work considers a discrete-time simulation with a fixed step Δt. At each time index k, the model evaluates the electrical values of the quadrotor propulsion system and advances the battery state. The model states are SoC_k, $V_{S,k}$, and $V_{L,k}$. The inputs are the commanded rotor speeds and torques $\{\omega_{k,i}; Q_{F,k,i}\}_{i=1}^{N}$, and flight controller $I_{FCS,k}$ and payload $I_{P,k}$ load currents. The model parameters (Table I) are taken from datasheets: motor constants K_V, K_F, R_m; ESC loss parameters R_{ON}, t_{ON}, t_{OFF} and switching frequency f; battery ECM parameters R_0, R_S, C_S, R_L, C_L, OCV polynomial coefficients $\{v_i\}_{i=0}^{7}$, and cell topology.

Figure 1 illustrates the logical and computational scheme of the energy consumption model, with arrows indicating the flow of the results from previous submodels to subsequent ones. It also represents the current flow of consumption from consumers to the battery.

This comprehensive, discrete-time model effectively integrates mechanical, electrical, and electrochemical components, explicitly accounting for nonlinear battery behavior, ESC switching losses, and motor dynamics. The simplifying assumptions – such as neglecting thermal effects, constant payload, and flight control system currents – limit the model to scenarios where these effects are minor. The model offers a balanced trade-off between complexity and practical utility.

The remaining limitations include:

- The need for rotor torque as an input is difficult to measure directly and must be estimated via indirect aerodynamic models.
- The exclusion of thermal and high-frequency magnetic effects limits model accuracy under extreme operating conditions.
- This model requires $\{\omega_{k,i}; Q_{F,k,i}\}_{i=1}^{N}$ as inputs; these are typically produced by an aerodynamic/propeller model or identified from thrust tables.
- The electrical model is intentionally decoupled from aerodynamics; therefore, overall accuracy depends on the external torque/speed estimator.

The proposed model intentionally simulates only the electrical domain and requires mechanical inputs $\{\omega_{k,i}; Q_{F,k,i}\}_{i=1}^{N}$. Aerodynamic coupling effects – such as induced inflow variations in forward flight, rotor–rotor interaction, and other effects – are not modeled inside the electrical module. This enables the latter to be used with an aerodynamic model of any level of complexity and accuracy. Therefore, the overall prediction accuracy depends on the fidelity of the external aerodynamic model used to provide accurate inputs.

IV. NUMERICAL SIMULATION

A. Simulation Methodology and Parameters

Simulations were conducted using publicly available real-world data and hardware specifications. Real-world flight data were taken from the NeuroBEM dataset [21], which provides time series for rotor speeds and thrust forces across various trajectories. For torque estimation, propeller performance data from [22] were used, matching the most compatible propulsion system combination employed in the dataset – APC BD5x3.7E-3-B4 propeller, DYS Samguk Wei 2207 2600 kV BLDC motor, and Hobbywing XRotor25A ESC. The 4S2P INR18650-20R battery cell with 14.8 V, 4000 mAh was selected due to the availability of open-access datasets [23] and detailed specifications [24], which enabled accurate parameter extraction for the second-order battery model (Table I).

Two EPS model versions were evaluated over three selected trajectories from NeuroBEM: one using a simplified battery model with a constant nominal voltage and capacity, and the other employing a second-order Thévenin ECM. The simulation assumed a fully charged battery (initial SoC=1). Each simulation follows a consistent protocol: the virtual flight begins with a fully charged battery and follows a closed-loop trajectory until the battery is fully discharged or its voltage falls below a specified threshold.

TABLE I. SIMULATION PARAMETERS

Symbol	Value and unit	Symbol	Value and unit
K_V	2600 rpm/V	C_n	*4000 mAh*
K_F	272.2 A/(Nm)	R_0	*20 mOhm*
R_m	50 mOhm	R_S	*10 mOhm*
R_{ON}	3.6 mOhm	C_S	*2500 F*
t_{ON}	45ns	R_L	*10 mOhm*
t_{OFF}	42ns	C_L	*7400 F*
f	16kHz	$\{v_i\}_{i=0}^{7}$	{84.6, -349, 592, -534, 275, -80.3, 12.8, 2.7}

The purpose of the experiments is to assess: 1) the accuracy of the proposed model in predicting power consumption under time-varying load conditions; 2) the difference in simulation results between the simplified and Thévenin battery models; 3) the model's capability to capture nonlinear and transient electrical phenomena.

B. Simulation Results

To validate the accuracy of the motor and ESC submodels, the simulation results were compared against experimental data from the equivalent hardware (closest available) in the Tyto Robotics database [25]. Figure 2 shows a close match between the modeled and experimental motor load current performance curves. The RMSE of motor load current (A), expressed as % of range/mean across the full rotational speed range, was 6.83%, whereas within the primary operating range (9000–21000 rpm), the RMSE was reduced to 3.07%. The remaining discrepancies can be attributed to a simplified BLDC motor model.

The NeuroBEM dataset includes various data-rich flight sequences. Three different trajectories were selected for simulation:

- Lemniscate: average velocity 1.68 m/s, duration 29 s, rotor speed range 10,000–12,300 rpm (file: 2021-02-23-10-48-03_seg_2).
- Circular path: average velocity 5.75 m/s, duration 32 s, rotor speed range 9,750–18,850 rpm (file: 2021-02-03-17-04-15_seg_3).
- Melon-shaped trajectory: average velocity 4.20 m/s, duration 59 s, rotor speed range 8,430–17,300 rpm (file: 2021-02-05-15-04-42_seg_2).

Simulation parameters are summarized in Table I. Motor specifications were derived from manufacturer datasheets. ESC characteristics were taken from [16], in which the authors reverse-engineered and characterized internal components. Battery parameters were obtained from [23, 24].

The simulation results for each trajectory are presented in Figure 3. The model parameters are listed in Table I, and the mechanical inputs are taken from the selected NeuroBEM dataset flights. Each trajectory is shown on a separate plot, with two dual-axis graphs per figure. The first pair of curves represents the total current consumed by the EPS, including all four motors and ESCs. These are shown as a red-green curve for the Thévenin model and a blue-yellow curve for the simplified battery model; alternating colors indicate cyclic patterns (trajectory repetition). The second pair of blue curves corresponds to the battery's SoC, with the Thévenin model depicted as a solid line and the fixed-voltage model as a dashed line. Quantitative simulation results are outlined in Table II, where the result ratio column shows the percentage values of the constant battery model compared to the Thévenin battery model. Based on the reported numerical indicators, the second-order Thévenin model provides superior accuracy in capturing the nonlinear processes associated with battery discharge, making it more suitable for dynamic simulations and endurance prediction.

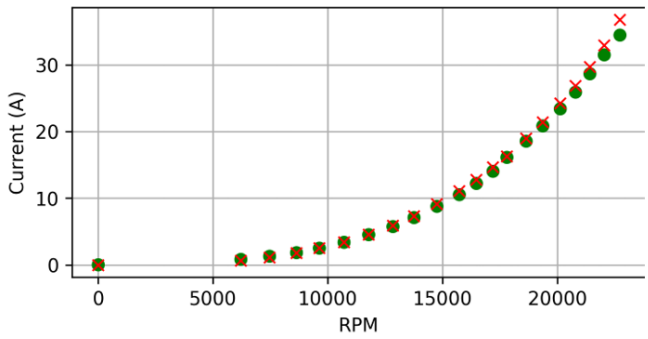

Fig. 2. Validation of the motor – ESC load current model with Tyto Robotics bench-test data: simulated (red) and experimental (green) motor AC load current I_{MAC} as a function of rotor speed $\omega_{k,i}[rpm]$.

TABLE II. SUMMARY METRICS FOR CONSTANT-VOLTAGE BASELINE VERSUS THÉVENIN BATTERY MODEL

Trajectory name	Metric	Constant battery	Thévenin battery	Result ratio, %
Lemniscate	Max current, A	12.33	18.98	65.0
	Mean current, A	11.67	12.44	93.8
	Flight time, s	1232.6	1155.9	106.6
Circular	Max current, A	52.9	86.65	61.1
	Mean current, A	22.30	25.88	86.2
	Flight time, s	645.2	531.5	121.4
Melon-shaped	Max current, A	41.3	78.9	52.3
	Mean current, A	17.1	19.3	88.6
	Flight time, s	842.8	743.7	113.3

C. Simulation Results Discussion

The proposed energy consumption model incorporates only parameters available from the manufacturer specifications (Table I), making it practical and transferable. The simulation of the ESC and motor, with torque values derived from propeller efficiency tables [22], demonstrates that the model accurately captures the electrical dynamics observed in experimental datasets. This confirms that the model accounts for the internal electrical behavior of both the ESC and motor subsystems.

The model's key advantage lies in integrating all electrical subsystems – battery, ESC, and motor – under a unified simulation framework. Its inputs, limited to rotor torque and angular velocity, allow compatibility with various kinematic and aerodynamic UAV models.

The numerical results demonstrate the limitations of simplified battery models. As depicted in Table II, fixed-voltage models consistently overestimate available onboard energy. The Thévenin model predicts shorter mission durations by 80–110 s (6–21%), depending on trajectory dynamics. This discrepancy could result in premature mission termination due to underestimated power limits. Simulation plots (Figure 3) further reveal dynamic behavior, such as increased current demand during a voltage sag, a feedback loop that accelerates energy depletion. This is especially evident in high-demand trajectories (e.g., the "Circular" path), where the ESC is unable

to maintain the expected power output under low-voltage conditions.

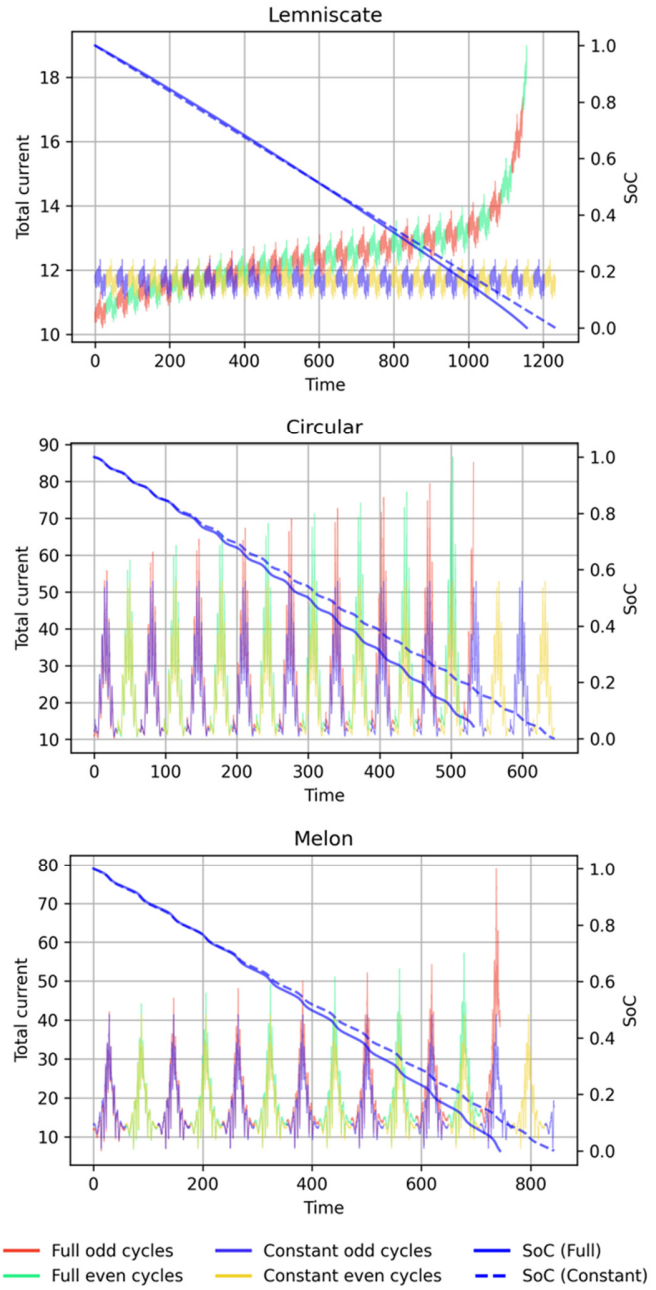

Fig. 3. Simulation results for three NeuroBEM trajectories (Lemniscate, Circular, Melon-shaped): propulsion current and battery state-of-charge versus time [s]. Simulation conditions from Table I.

Validation against real-flight or dedicated bench measurements would further strengthen the current study. However, conducting controlled flight experiments and instrumentation was not feasible within the scope of this work due to resource and funding limitations, while no publicly available dataset containing the required data was identified. Therefore, the present validation compares the proposed framework against the widely used constant-voltage baseline to isolate the effect of modeling internal electrical losses. The lack of real-flight validation is explicitly stated as a limitation and is planned as future work.

The code and simulation data can be found and reproduced in [26].

V. CONCLUSIONS

Unlike the models previously proposed, the analytical model developed in this study explicitly incorporates the energy consumption of both the flight control system and the payload, as well as a detailed representation of every component within the electrical propulsion subsystem, including battery, Electronic Speed Controller (ESC), and Brushless Direct Current (BLDC) motors. This comprehensive, discrete-time formulation accounts for nonlinear battery dynamics, ESC switching losses, and motor electromechanical behavior, enabling precise simulation and analysis. Although certain simplifying assumptions – such as neglecting thermal effects and treating payload and flight control currents as constants – limit the model's scope, future work can extend this framework by incorporating dynamic payload variations, thermal effects, and variable flight control consumption for enhanced accuracy and broader applicability.

A primary area for future work is the experimental validation of the model using synchronized onboard logs of $V_B(t)$, $I_B(t)$, rotor speed/throttle, and mission profiles. This was not feasible within the present study, and no suitable open dataset was identified; therefore, comprehensive real-flight validation is left for follow-up work. Additional research may also focus on incorporating extended nonlinearities (e.g., temperature and aging) to broaden the applicability of the proposed model in long-duration and high-stress UAV missions.

REFERENCES

[1] N. Delavarpour, C. Koparan, J. Nowatzki, S. Bajwa, and X. Sun, "A Technical Study on UAV Characteristics for Precision Agriculture Applications and Associated Practical Challenges," *Remote Sensing*, vol. 13, no. 6, 2021, Art. no. 1204, https://doi.org/10.3390/rs13061204.

[2] T. P. F. Sompie, R. E. Makangiras, J. A. J. Sumajouw, and C. Hombokau, "Application of Unmanned Aerial Vehicle and Ground Control Point for Mapping and Road Geometric Review: A Case Study: Pandu – Kima Atas Street," *Engineering, Technology & Applied Science Research*, vol. 14, no. 4, pp. 15986–15992, Aug. 2024, https://doi.org/10.48084/etasr.8040.

[3] S. P. H. Boroujeni *et al.*, "A comprehensive survey of research towards AI-enabled unmanned aerial systems in pre-, active-, and post-wildfire management," *Information Fusion*, vol. 108, Aug. 2024, Art. no. 102369, https://doi.org/10.1016/j.inffus.2024.102369.

[4] C. Muli, S. Park, and M. Liu, "A Comparative Study on Energy Consumption Models for Drones," in *5th Global IoT Summit* (*GIoTS*), Dublin, Ireland, June 20–23, 2022, pp. 199–210, https://doi.org/10.1007/978-3-031-20936-9_16.

[5] W. Dai, M. Zhang, and K. H. Low, "Data-efficient modeling for power consumption estimation of quadrotor operations using ensemble learning," *Aerospace Science and Technology*, vol. 144, Jan. 2024, Art. no. 108791, https://doi.org/10.1016/j.ast.2023.108791.

[6] H. V. Abeywickrama, B. A. Jayawickrama, Y. He, and E. Dutkiewicz, "Comprehensive Energy Consumption Model for Unmanned Aerial Vehicles, Based on Empirical Studies of Battery Performance," *IEEE*

Access, vol. 6, pp. 58383–58394, 2018, https://doi.org/10.1109/ACCESS.2018.2875040.

[7] A. Abdilla, A. Richards, and S. Burrow, "Power and endurance modelling of battery-powered rotorcraft," in *2015 IEEE/RSJ International Conference on Intelligent Robots and Systems* (*IROS*), Hamburg, Germany, Sept. 28–2, 2015, pp. 675–680, https://doi.org/10.1109/IROS.2015.7353445.

[8] H. Yan, Y. Chen, and S.-H. Yang, "New Energy Consumption Model for Rotary-Wing UAV Propulsion," *IEEE Wireless Communications Letters*, vol. 10, no. 9, pp. 2009–2012, Sept. 2021, https://doi.org/10.1109/LWC.2021.3090772.

[9] Y. Zeng, J. Xu, and R. Zhang, "Energy Minimization for Wireless Communication With Rotary-Wing UAV," *IEEE Transactions on Wireless Communications*, vol. 18, no. 4, pp. 2329–2345, Apr. 2019, https://doi.org/10.1109/TWC.2019.2902559.

[10] H. Gong, B. Huang, B. Jia, and H. Dai, "Modeling Power Consumptions for Multirotor UAVs," *IEEE Transactions on Aerospace and Electronic Systems*, vol. 59, no. 6, pp. 7409–7422, Dec. 2023, https://doi.org/10.1109/TAES.2023.3288846.

[11] C. W. Chan and T. Y. Kam, "A procedure for power consumption estimation of multi-rotor unmanned aerial vehicle," *Journal of Physics: Conference Series*, vol. 1509, no. 1, Dec. 2020, Art. no. 012015, https://doi.org/10.1088/1742-6596/1509/1/012015.

[12] F. Yacef, N. Rizoug, L. Degaa, O. Bouhali, and M. Hamerlain, "Trajectory optimisation for a quadrotor helicopter considering energy consumption," in *4th International Conference on Control, Decision and Information Technologies* (*CoDIT*), Barcelona, Spain, Apr. 5–7, 2017, pp. 1030–1035, https://doi.org/10.1109/CoDIT.2017.8102734.

[13] M. Jacewicz, M. Żugaj, R. Głębocki, and P. Bibik, "Quadrotor Model for Energy Consumption Analysis," *Energies*, vol. 15, no. 19, 2022, Art. no. 7136, https://doi.org/10.3390/en15197136.

[14] R. Głębocki, M. Żugaj, and M. Jacewicz, "Validation of the energy consumption model for a quadrotor using Monte-Carlo simulation," *Archive of Mechanical Engineering*, vol. 70, no. 1, pp. 151-178, 2023, https://doi.org/10.24425/ame.2022.144075.

[15] Y. Wang *et al*., "Multiobjective Energy Consumption Optimization of a Flying–Walking Power Transmission Line Inspection Robot during Flight Missions Using Improved NSGA-II," *Applied Sciences*, vol. 14, no. 4, 2024, Art. no. 1637, https://doi.org/10.3390/app14041637.

[16] J. Jeong, H. Shi, K. Lee, and B. Kang, "Improvement of Electric Propulsion System Model for Performance Analysis of Large-Size Multicopter UAVs," *Applied Sciences*, vol. 10, no. 22, 2020, Art. no. 8080, https://doi.org/10.3390/app10228080.

[17] M. Chen and G. A. Rincon-Mora, "Accurate electrical battery model capable of predicting runtime and I-V performance," *IEEE Transactions on Energy Conversion*, vol. 21, no. 2, pp. 504–511, June 2006, https://doi.org/10.1109/TEC.2006.874229.

[18] J. Li, Y. Wang, R. M. G. Ferrari, J. Swevers, and F. Ding, "Online Lithium-ion Battery Modeling and State of Charge Estimation via Concurrent State and Parameter Estimation∗," *IFAC-PapersOnLine*, vol. 58, no. 15, pp. 462–467, 2024, https://doi.org/10.1016/j.ifacol.2024.08.572.

[19] D. Lundström, K. Amadori, and P. Krus, "Validation of Models for Small Scale Electric Propulsion Systems," in *48th AIAA Aerospace Sciences Meeting Including the New Horizons Forum and Aerospace Exposition*, Orlando, Florida, Jan. 4–7, 2010, https://doi.org/10.2514/6.2010-483.

[20] Mark Drela, "First-Order DC Electric Motor Model," https://web.mit.edu/drela/Public/web/qprop/motor1_theory.pdf.

[21] L. Bauersfeld, E. Kaufmann, P. Foehn, S. Sun, and D. Scaramuzza, "NeuroBEM: Hybrid Aerodynamic Quadrotor Model," in *Robotics: Science and Systems XVII*, online, July 12–16, 2021, https://doi.org/10.15607/RSS.2021.XVII.042.

[22] "Performance Data." APC Propellers. https://www.apcprop.com/technical-information/performance-data/.

[23] "Battery Data." Center for Advanced Life Cycle Engineering. https://calce.umd.edu/battery-data.

[24] "Test of Samsung INR18650-20R 2000mAh (Green)." https://lygte-info.dk/review/batteries2012/Samsung%20INR18650-20R%202000mAh%20%28Green%29%20UK.html.

[25] Rob Hessler. "DYS Samguk Wei Azure Power 5150 test data." https://database.tytorobotics.com/tests/9ym/dys-samguk-wei-azure-power-5150.

[26] *vadyusikh/uav_eecn*. (2025) V. Honcharenko. [Online]. Available: https://github.com/vadyusikh/uav_eecn.